

PAPER

Electronic correlations in uranium hydride UH_5 under pressure

To cite this article: Alexey O Shorikov *et al* 2020 *J. Phys.: Condens. Matter* **32** 385602

View the [article online](#) for updates and enhancements.



IOP | ebooks™

Bringing together innovative digital publishing with leading authors from the global scientific community.

Start exploring the collection—download the first chapter of every title for free.

Electronic correlations in uranium hydride UH₅ under pressure

Alexey O Shorikov^{1,2,3} , Sergey L Skornyakov^{1,2,3} , Vladimir I Anisimov^{1,2,3}  and Artem R Oganov³ 

¹ M N Mikheev Institute of Metal Physics of the Ural Branch of the Russian Academy of Sciences, Yekaterinburg 620108, Russia

² Department of Theoretical Physics and Applied Mathematics, Ural Federal University, 19 Mira St., Yekaterinburg 620002, Russia

³ Skolkovo Institute of Science and Technology, 3 Nobel Street, Moscow 143026, Russia

E-mail: shorikov@imp.uran.ru

Received 17 March 2020, revised 3 May 2020

Accepted for publication 22 May 2020

Published 19 June 2020



Abstract

We report results of calculations based on density functional theory and dynamical mean-field theory for the electronic structure of uranium hydride UH₅ under pressure, a compound of the uranium-based hydride family some members of which have been predicted to be superconducting. The effective electronic mass enhancement $m^*/m \sim 1.4$ indicates that the Coulomb correlations have a moderate strength. However, the topology of the Fermi surface changes strongly at the influence of the correlation effects: one hourglass-like pocket running along the Γ - A direction splits into two elliptical pockets centered at the A point. This result shows the possibility of an unconventional pairing mechanism for uranium hydrides in addition to the electron-phonon pairing that was studied in previous investigations.

Keywords: uranium hydrides, electron correlation effects, Lifshitz transition, high pressure

(Some figures may appear in colour only in the online journal)

1. Introduction

Superconductivity is considered to be one of the most interesting topics of condensed matter physics, and its practical application is very important for industry. The explanation of this effect, observed in many metals and compounds, has been proposed in the revolutionary work of Bardeen, Cooper and Schrieffer (BCS) [1]. First superconductors demonstrated the s -wave symmetry of the order parameter that has been introduced in [2]. The discovery of high- T_c superconductivity in layered cuprates [3] has drastically changed the field. An important observation has been made in an experiment that indicated the d -wave symmetry of the order parameter and singlet Cooper pairing [4]. It has been found that the Coulomb correlations are responsible for many unusual properties of high- T_c cuprates: the temperature dependence of the electrical resistivity, non-Fermi liquid behavior, and so forth. A new class of layered iron-based pnictides [5] with a relatively

high superconducting temperature has sparked the interest due to their difference from cuprates. While the latter are doped Mott insulators whose physics can be described using a single electronic band, the pnictides are semimetals with a complex multiband structure near the Fermi level. For iron pnictides, the importance of the correlation effects for superconductivity has been investigated [6, 7].

The lightest chemical element hydrogen is expected to exhibit superconductivity with a high transition temperature T_c under strong compression because of a very strong electron-phonon coupling, which has been proposed for metallic hydrogen decades ago [8, 9]. Although not confirmed in experiment because the necessary pressure, which exceeds 400 GPa, lies beyond the capability of modern experimental techniques, high T_c of metallic hydrogen has been predicted in several electronic structure calculations [10, 11]. It has been found that the H-H distance necessary for the metallization of molecular hydrogen can be achieved at lower pressures in a

hydrogen-rich compound. This field experiences renaissance after conventional superconductivity was predicted and then confirmed experimentally for H_3S under high pressure [12, 13]. Recently, superconductivity was predicted in lanthanum and yttrium hydrides [14, 15]. For LaH_{10} , the calculated transition temperature $T_c = 274\text{--}286$ K at 210 GPa; for YH_{10} , $T_c = 305\text{--}326$ K at 250 GPa. Both LaH_{10} and YH_{10} were found to be metals with large densities of states at the Fermi level and with the electron–phonon superconductivity mechanism. The f- and d-states of rare-earth metals make a significant contribution to the density of states at the Fermi level and the role of the La and Y atoms is still under debate: do they simply stabilize the clathrate hydrogen structure or induce complex reconstruction of band structure at Fermi level and hence make an impact on superconductivity. The calculations made for a model crystal substructure of LaH_{10} without the La atoms (the so-called Cs-IV structure) have demonstrated an even higher transition temperature of ~ 300 K but at substantially higher pressure 300 GPa [16]. Hydrogen-rich compounds have attracted great attention and have been the topic of much research. However, they have not been considered potential candidates for practical use because superconductivity in them occurs at very high pressures.

Superconductivity has also been found in many uranium compounds that demonstrate heavy-fermion behavior. The well-known member of this series UBe_{13} with $T_c = 0.86$ K [17] has the electronic mass enhancement factor $m^*/m \sim 10^3$, which speaks for the importance of correlations. However, a closer look into the crystal structure has revealed more differences than similarities between rare-earth hydrides and UBe_{13} because the latter is an intermetallic compound in which the U atoms can be viewed as impurities in the metallic Be solvent.

The stability of uranium hydrides has been recently investigated within the DFT framework [18]. As a result, 14 new stable compounds have been predicted, including hydrogen-rich UH_5 , UH_6 , U_2H_{13} , UH_7 , UH_8 , U_2H_{17} , and UH_9 ; stability has been confirmed experimentally for UH_7 , UH_8 , and three phases of UH_5 . Many of the predicted phases are expected to be superconductors [18]. The crystal structures of these UH_x compounds resemble lanthanum-based hydrides where an f-metal is placed in the center of the hydrogen cage. The similarity of crystal structures suggests that the mechanism of superconductivity could be the same as in lanthanum polyhydrides and the main role of the U atoms is the stabilization of the crystal structure. But, unlike the La-based hydrides where the f-shell of the central atom is empty, uranium has a partially filled f-shell that forms narrow bands crossing the Fermi level. This suggests that the Coulomb correlations could be important and, in addition to the electron–phonon coupling, another pairing mechanism should be considered.

In this paper, we explore the Coulomb correlation effects in UH_5 . For this compound, DFT calculations produce a rather strong peak, formed by the 5f-states of uranium, in the density of states close to the Fermi energy, which usually suggests the presence of significant correlation effects. Using the state-of-the-art DFT + DMFT method [19, 20], we calculated the electronic band structure of UH_5 and compared its spectral properties with those predicted by density functional theory.

Our results reveal a strong influence of the correlation effects on the Fermi surface and the renormalization of the band mass m^*/m . We obtained $m^*/m \sim 1.4$, indicating moderate correlation effects in UH_5 . Upon the inclusion of the local Coulomb interaction, we observed a topological transition of the Fermi surface along the $\Gamma\text{--}A$ direction of the hexagonal Brillouin zone. Our results highlight the effect of electronic correlations in UH_5 and clearly show the sensitivity of its low-energy electronic structure to the local Coulomb interactions between the electrons of the partially filled shells. These observations allow us to suggest that, along with the standard phonon-based mechanism, an unconventional electron pairing may mediate superconductivity of UH_x compounds.

2. Computational details

To study the electronic structure of UH_5 , we used the DFT + DMFT method [20, 21]. This approach has been shown to describe a complex interplay of electronic and magnetic properties of strongly correlated materials under pressure [22, 23]. The calculations were performed in three steps. First, the non-interacting band structure was computed using DFT. We used the GGA (generalized gradient approximation) [24] as implemented in the Quantum Espresso package [25]. Second, an effective Hamiltonian H_{DFT} was constructed on the basis of the atomic-centered Wannier functions using the projection procedure [26]. Due to the mixed character of the electronic states of UH_5 near the Fermi level, we used an energy window spanning the U-s, -d, -f, and H-s bands.

Finally, the full many-body Hamiltonian to be solved using DFT + DMFT has the form:

$$\hat{H} = \hat{H}_{\text{DFT}} - \hat{H}_{\text{DC}} + \frac{1}{2} \sum_{i,m,m',\sigma,\sigma'} U_{m,m'}^{\sigma,\sigma'} \hat{n}_{i,m,\sigma} \hat{n}_{i,m',\sigma'}. \quad (1)$$

Here, $U_{m,m'}^{\sigma,\sigma'}$ is the Coulomb interaction matrix and $\hat{n}_{i,m,\sigma}$ is the occupation number operator for the f electrons with orbital and spin indices i, m, σ at the i th site. The elements of $U_{m,m'}^{\sigma,\sigma'}$ matrix were parameterized by the on-site Hubbard parameter U and Hund's intra-atomic exchange J_{H} according to the procedure described in reference [27]. In our calculations we set $U = 4$ eV and $J_{\text{H}} = 0.5$ eV. The term \hat{H}_{DC} stands for the so-called double-counting correction, that is the f–f interaction energy already accounted for in DFT. We chose the double-counting correction in the form $\hat{H}_{\text{DC}} = \bar{U}(N_f - \frac{1}{2})\hat{I}$ [20]. Here N_f is the total self-consistent number of f electrons obtained within DFT + DMFT, \bar{U} is the average Coulomb parameter for the f-shell, and \hat{I} is the identity operator. The effective DMFT impurity problem was solved by the hybridization expansion of continuous-time quantum Monte-Carlo method (CT-QMC) [28] as implemented in the AMULET package [29]. The QMC calculations were performed for the paramagnetic state at electronic temperatures $T = 1160$ K, 580 K, 300 K and 232 K ($\beta = 10$ eV $^{-1}$, 20 eV $^{-1}$, 38 eV $^{-1}$ and 50 eV $^{-1}$) and for FM and AFM state at $T = 1160$ K ($\beta = 10$ eV $^{-1}$). To compute the spectral properties and renormalizations of the quasiparticle mass, we used the real-axis

self-energy $\hat{\Sigma}(\omega)$ obtained by the Padé analytical continuation procedure [30].

3. Results and discussion

We started by performing the electronic structure calculations of UH_5 using the hexagonal crystal structure at 20 GPa proposed in reference [18]. According to the original predictions [18], among uranium hydrides only UH_3 and UH_5 are magnetic (and indeed, our calculations indicate high DOS at the Fermi level, and Stoner instability which can result in ferromagnetism). Magnetism of these compounds means that they are more correlated than hydrides predicted to be superconducting such as UH_7 , and sets an upper bound for the importance of electronic correlations in such compounds. Using DFT + DMFT we checked long-range FM and AFM orders for UH_5 and found that it remains paramagnetic at 1100 K but with a sizable value of the instant squared magnetic moment $\langle m_z^2 \rangle = 3.1 \mu_B^2$ implying the presence of magnetic fluctuations. This indicates that some long-range magnetic order could be stable at lower temperatures.

The results for the momentum-integrated spectral functions computed within both DFT and DFT + DMFT are shown in figure 1. The total DFT spectral function of UH_5 corresponds to a metal with a large value of the density of states at the Fermi level. The shape of the spectral function in the vicinity of the Fermi energy E_F results mostly from the U-f contribution. These states form a rather narrow partially filled band localized in the interval from -0.5 to 1.5 eV with a sharp peak at ~ 0.1 eV above the Fermi level. By contrast, the H-s states form a much broader band starting at -6 eV and spanning the energies far above E_F . We observed that the U-f and H-s bands are not separated and strongly hybridize. This electronic structure is similar to that of the parent compounds of superconducting iron pnictides and chalcogenides [31, 32] and very different from that of oxides and perovskites with well-separated metal and oxygen bands [33, 34]. The H-s spectral function shows a bonding-antibonding splitting, with bonding states separated from the antibonding subband by a gap of ~ 0.5 eV. The peak of the H-s symmetry close to E_F has a much smaller amplitude than one of the U-f symmetry and is presumably a symmetry of the s-f hybridization.

The shapes of the spectral functions obtained using DFT + DMFT (figure 1, solid lines) and DFT (figure 1, shaded areas) are similar in general. However, the effect of correlations is seen as a significant modification of the low-energy bands. The strongest transformation occurs in the U-f spectral functions where the correlation effects shift and renormalize the states close to the Fermi level. In particular, a sharp peak located at ~ 0.1 eV in DFT emerges almost right at the Fermi level in DFT + DMFT. The correlations are not strong enough to induce a significant transfer of the spectral weight. For example, a broad feature in the interval from -3 to -1 eV is caused by the s-f hybridization and should not be mistaken with the lower Hubbard band. The H-s spectral function shows only an insignificant broadening, presumably because of the temperature and hybridization effects. The observed effect

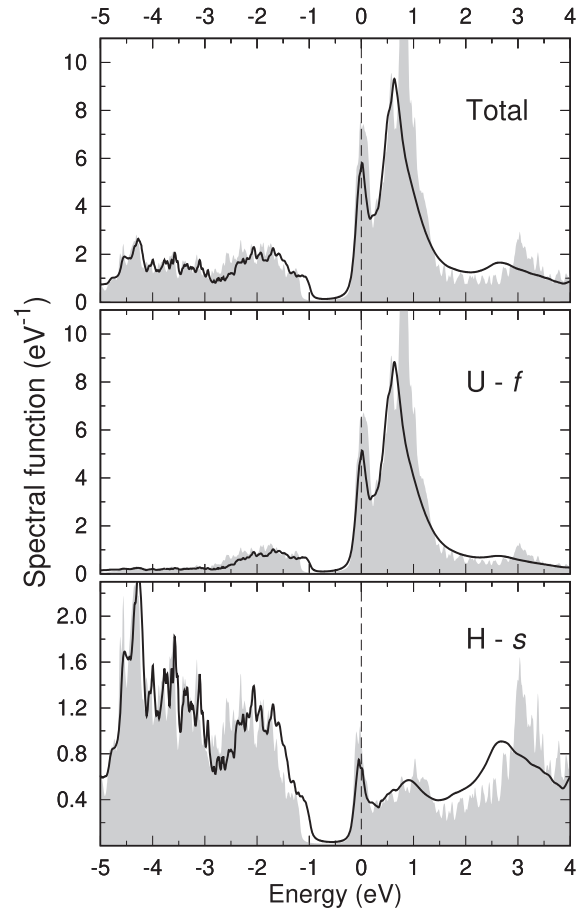


Figure 1. The total (top), U-f (center), and H-s (bottom) spectral functions of UH_5 calculated at $T = 232$ K using the DFT + DMFT (solid lines) and DFT (shaded areas).

of electronic correlations on the electronic structure of UH_5 resembles the one found in the iron pnictide superconductors [31, 35].

The results for the U-f orbitally resolved spectral functions $A_j(\omega)$ are shown in figure 2. Here f_1, \dots, f_7 label linear combinations of f Wannier states constructing a diagonal representation of the local occupation matrix. Therefore, these states cannot be called standard f-cubic harmonics. Also presented is the frequency dependence of the corresponding diagonal elements of the local electronic self-energies $\text{Im} \hat{\Sigma}_{jj}(i\omega_n)$ computed using DFT + DMFT. The comparison of the DFT and DFT + DMFT results shows that $A_j(\omega)$ exhibit a similar scaling transformation caused by the correlation effects for all U-f orbitals. The self-energies of the orbitals with sharp peaks in $A_j(\omega)$ at $E_F - f_2, f_3$, and f_7 —display the largest nonzero value for $i\omega \rightarrow 0$, whereas those of the other orbitals (f_1, f_4, f_5 , and f_6) remain Fermi liquid-like. The coexistence of states with a high and low electronic coherence may indicate orbital-dependent effects occurring in UH_5 under pressure (e.g., the orbital-selective formation of local moments).

To proceed further, we calculate the local spin-spin correlation function $\langle \mathbf{S}_z(\tau) \mathbf{S}_z(0) \rangle$ which shape and amplitude characterizes the lifetime of the local moment. Namely, if magnetic moments are localized, $\langle \mathbf{S}_z(\tau) \mathbf{S}_z(0) \rangle$ is constant: $\approx S^2$ and

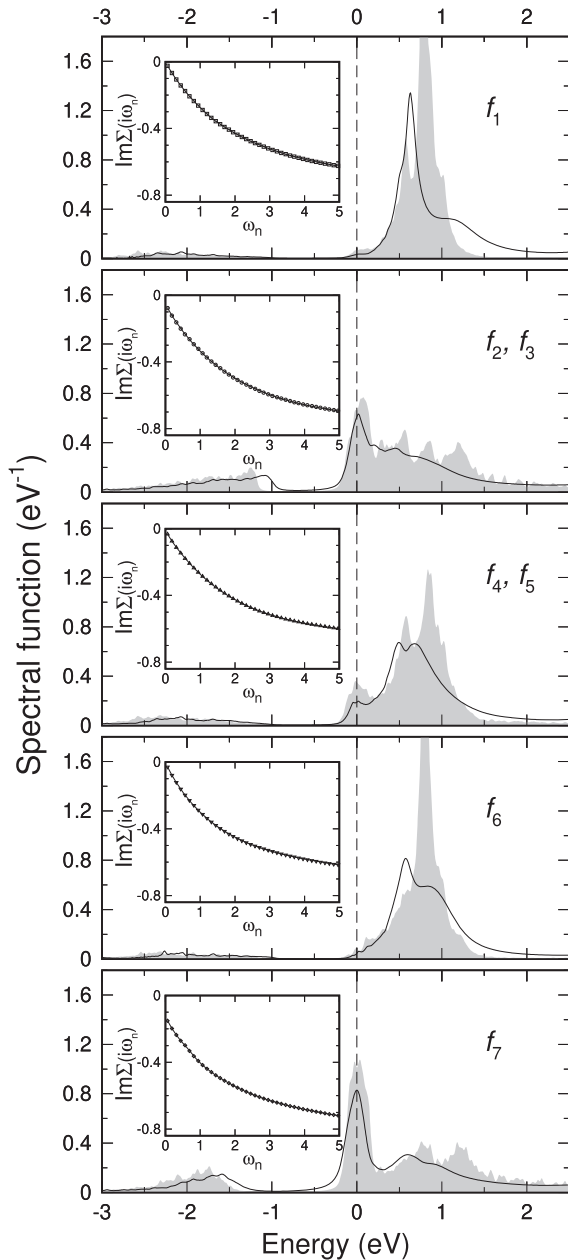


Figure 2. The orbitaly resolved U-f spectral functions of UH₅ calculated at $T = 232$ K using DFT + DMFT (solid lines) and DFT (shaded areas). The corresponding orbital projections of the DFT + DMFT self-energy on the Matsubara mesh are shown in the insets. The Fermi energy (0 eV) is shown by a dashed line.

drops rapidly with τ if electrons are delocalized (i.e. Fermi-liquid regime). This difference in the behavior of correlation function can be seen for two groups of f-orbitals on figure 3. The temperature dependence of this correlation function could be used as the measure of localization degree e.g. in Fermi-liquid regime $\langle \mathbf{S}_z(\tau) \mathbf{S}_z(0) \rangle \sim T^2 / \sin(\tau\pi T)^2$ [36] for τ far enough from 0 and β and should be temperature independent if electrons are fully localized. The $\langle \mathbf{S}_z(\beta/2) \mathbf{S}_z(0) \rangle$ shown in the inset of figure 3 is a linear function of T^2 for $f_1, f_4, f_5,$ and f_6 orbitals which indicates Fermi-liquid regime i.e. delocalization. In contrast the behavior of this correlation function for $f_2, f_3,$ and f_7 is more complex (neither proportional to T^2 nor

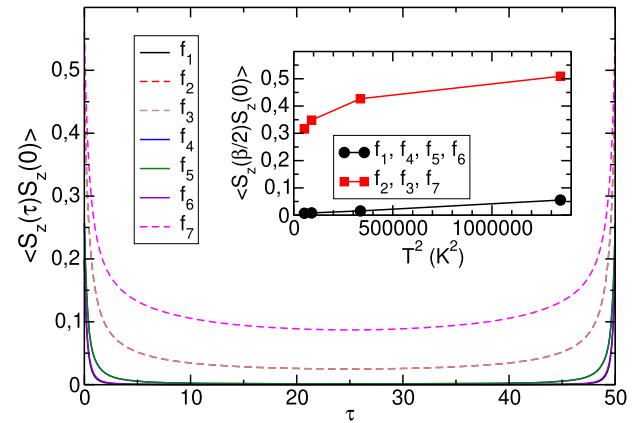


Figure 3. Spin-spin correlation function for different f-WF. The inset shows the dependence of the spin-spin correlation function on T^2 for two types of orbitals.

Table 1. Orbitaly resolved enhancement of the band mass m^*/m in UH₅ for different orbitals of the f-shell calculated within DFT + DMFT at $T = 387$ K.

	f_1	f_2, f_3	f_4, f_5	f_6	f_7
m^*/m	1.37	1.39	1.38	1.44	1.31

a constant) indicative of the intermediate regime with partially localized electrons.

Next, we computed the band mass enhancement $m^*/m = (1 - \frac{\partial \text{Re} \Sigma(\omega)}{\partial \omega} |_{\omega \rightarrow 0})$, which provides a quantitative measure of the correlation strength. The derivative $\frac{\partial \text{Re} \Sigma(\omega)}{\partial \omega} |_{\omega \rightarrow 0}$ was calculated using the Padé extrapolation of the self-energy $\Sigma(i\omega)$ to $\omega = 0$. The results (table 1) show that the electronic correlations have an approximately equal strength for all 4f-orbitals with m^*/m ranging from 1.31 to 1.44. By analogy with the classification scheme introduced for iron pnictides [31], this enhancement of the effective mass characterizes a regime of moderate electronic correlations. In such a case the correlation effects drive a significant renormalization of the band structure near the Fermi energy but are not sufficient to expel the spectral weight from the Fermi level and form the Hubbard bands.

To understand the effect of electronic correlations in more detail, we analyzed the momentum-resolved spectral properties of UH₅. The comparison of the DFT band structure with the spectral weight distribution along the high-symmetry lines in the hexagonal Brillouin zone computed using DFT + DMFT is presented in figure 4. For clarity, the contributions of the U-f and H-s states are shown separately. Both DFT and DFT + DMFT give a similar band structure with the spectral density in the vicinity of the Fermi energy originating mostly from the U-f states. However, the contribution of the H-s states at E_F is not negligible and is comparable with that of the U-f states along the Γ -A direction. The energy bands close to E_F show a pronounced dispersion in the entire Brillouin zone except the flat regions of mixed character along the Γ -A-L path. The weak dispersion of these bands presumably gives rise to a sharp peak of the spectral function in the part of the

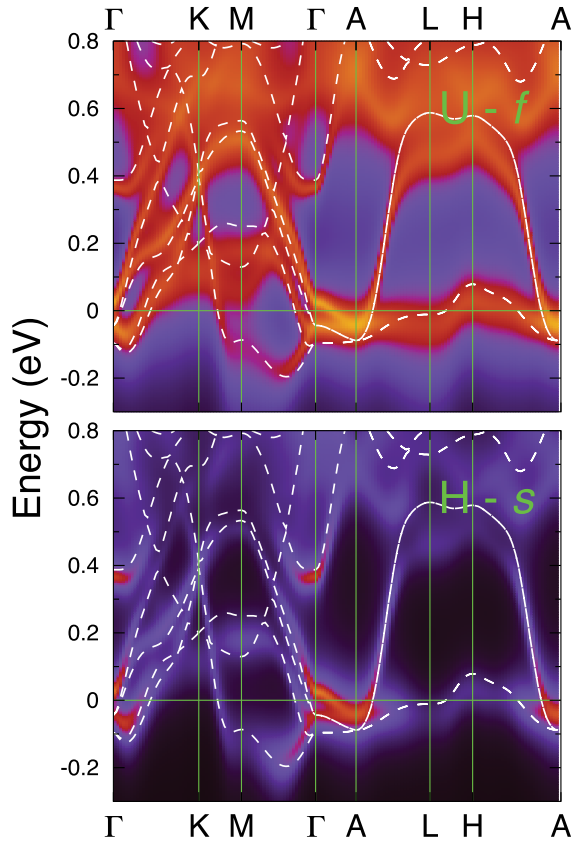


Figure 4. The momentum-resolved spectral function of the U-f (top) and H-s (bottom) states of UH_5 at $T = 232$ K computed using the DFT + DMFT. The DFT band structure is shown by dashed lines.

orbitals located above the Fermi level in DFT and almost right at E_F in DFT + DMFT. Most importantly, electronic correlations modify DFT band structure in a way that cannot be described as a simple scaling transformation. DFT + DMFT calculations show that the band of predominantly U-f character at the Γ point is pushed from below to above the Fermi level, resulting in the topological change of the Fermi surface along the Γ -A direction. The rest of the band structure close to E_F , including the bands with a strong contribution from the H-s states, is renormalized by a factor of m^*/m .

To further analyze how the electronic correlations modify the bands crossing the Fermi level, we compared the Fermi surfaces of UH_5 computed using DFT and DFT + DMFT. The latter is visualized by determining the poles of the DFT + DMFT lattice Green function. The DFT Fermi surface (figure 5, left) consists of two parts. The first (inner) Fermi surface is centered in the Γ -A direction and has an hourglass shape, its cross-section area in the (k_x, k_y) plane has a pronounced dependence on k_z . This Fermi surface pocket has a predominantly U-f character close to the Γ point and mixed s-f character at the zone border around the A point. The second Fermi surface has a complex shape resembling a six-tooth gear with a cut in the center and the axis parallel to the Γ -A direction. The ‘teeth’ are warped cylinders pointing to the M points and truncated by the faces of the hexagonal Brillouin zone. Unlike the inner hourglass-like pocket, the outer gear-like Fermi surface results mostly from the U-f bands.

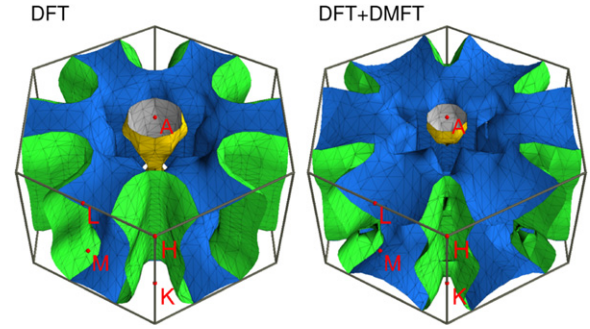


Figure 5. The Fermi surface of UH_5 at $T = 232$ K computed using DFT (left) and DFT + DMFT (right). Solid lines represent the hexagonal Brillouin zone.

A strong effect of electronic correlations is revealed in the Fermi surface computed using DFT + DMFT (figure 5, right). The deformation of the gear-like sheet leads to the emergence of pronounced convex and concave structures on its surface; however, the symmetry of this part of the Fermi surface is unaffected by correlations. By contrast, the inner hourglass-like Fermi surface closes off along the Γ -A direction and turns into two separate pockets encircling the A points of the Brillouin zone. In the iron chalcogenide compound FeSe , a similar transformation of the inner pocket by the (chemical) pressure and correlation effects (2D to 3D crossover) has been confirmed in both theory and experiment [32, 37]. The similar disagreement between ARPES experiment and DFT calculation for Na_xCoO_2 points to the importance of taking into account correlation effects: the DFT + U calculation showed the suppression of the hole pocket obtained using the DFT [38]. Overall, we found that in UH_5 under pressure the electron-electron interactions lead to a significant reduction of the parts of the Fermi surface derived from H-s, whereas the volume and the surface area of the sheets derived from U-f show a small increase compared to that predicted using the DFT.

4. Conclusions

Using the DFT + DMFT method, we investigated and quantified the effect of electronic Coulomb correlations on the electronic properties of uranium hydride UH_5 . The results demonstrate the importance of the correlation effects for the electronic band structure and the Fermi surface. We found a moderately strong enhancement of the band mass m^*/m in the range of 1.31 to 1.44 accompanied by a shift and renormalization of quasiparticle bands near the Fermi level and an absence of the Hubbard bands in the spectral function. By analogy with iron pnictide- and chalcogenide-based superconductors, we characterize UH_5 as a moderately correlated compound. Our results for the spectral properties reveal the correlation-induced transformation of the Fermi surface topology along the Γ -A direction leading to the formation of a closed pocket encircling the A points of the hexagonal Brillouin zone. Considering the presence of both H-s and U-f states at the Fermi level and the pronounced response of the f-derived bands to

electron–electron interactions, we speculate that superconductivity of uranium hydrides under pressure could be of mixed origins. This suggests that unconventional mechanisms of pairing should be treated on an equal footing with the standard BCS-type mechanism in a model describing superconductivity of UH_x .

Acknowledgments

The DFT calculations were performed within the state assignment of the Ministry of Science and Higher Education of Russia (Theme ‘Electron’ No. AAAA-A18-118020190098-5). The DFT + DMFT calculations were supported by the Russian Science Foundation (Project No. 19-72-30043).

ORCID iDs

Alexey O Shorikov  <https://orcid.org/0000-0001-7607-6130>
Sergey L Skornyakov  <https://orcid.org/0000-0001-8024-0917>

Vladimir I Anisimov  <https://orcid.org/0000-0002-1087-1956>

Artem R Oganov  <https://orcid.org/0000-0001-7082-9728>

References

- [1] Bardeen J, Cooper L N and Schrieffer J R 1957 *Phys. Rev. B* **108** 1175
- [2] Ginzburg V L and Landau L D 1950 *Zh. Eksp. Teor. Fiz.* **20** 1064
- [3] Bednorz J G and Müller K A 1986 *Z. Phys. B* **64** 189
- [4] Tsuei C C and Kirtley J R 2000 *Rev. Mod. Phys.* **72** 969
- [5] Kamihara Y, Hiramatsu H, Hirano M, Kawamura R, Yanagi H, Kamiya T and Hosono H 2006 *J. Am. Chem. Soc.* **128** 10012–3
- [6] Sadovskii M V 2008 *Phys.-Usp.* **51** 1201
- [7] Skornyakov S L, Skorikov N A, Lukoyanov A V, Shorikov A O and Anisimov V I 2010 *Phys. Rev. B* **81** 174522
- [8] Wigner E and Huntington H B 1935 *J. Chem. Phys.* **3** 764
- [9] Ashcroft N W 1968 *Phys. Rev. Lett.* **21** 1748
- [10] Cudazzo P, Profeta G, Sanna A, Floris A, Continenza A, Massidda S and Gross E K U 2010 *Phys. Rev. B* **81** 134506
- [11] McMahon J M and Ceperley D M 2011 *Phys. Rev. B* **84** 144515
- [12] McMahon J M and Ceperley D M 2012 *Phys. Rev. B* **85** 219902
- [13] Li Y, Hao J, Liu H, Li Y and Ma Y 2014 *J. Chem. Phys.* **140** 174712
- [14] Troyan I, Gavriuliuk A, Rüffer R, Chumakov A, Mironovich A, Lyubutin I, Perekalin D, Drozdov A P and Eremets M I 2016 *Science* **351** 1303–6
- [15] Liu H, Naumov I I, Hoffmann R, Ashcroft N W and Hemley R J 2017 *Proc. Natl Acad. Sci.* **114** 6990–5
- [16] Kruglov I A *et al* 2020 *Phys. Rev. B* **101** 024508
- [17] Liu H, Naumov I I, Geballe Z M, Somayazulu M, Tse J S and Hemley R J 2018 *Phys. Rev. B* **98** 100102
- [18] Ott H R, Rudigier H, Fisk Z and Smith J L 1983 *Phys. Rev. Lett.* **50** 1595
- [19] Kruglov I A *et al* 2018 *Sci. Adv.* **4** eaat9776
- [20] Georges A, Kotliar G, Krauth W and Rozenberg M J 1996 *Rev. Mod. Phys.* **68** 13
- [21] Anisimov V I, Poteryaev A I, Korotin M A, Anokhin A O and Kotliar G 1997 *J. Phys.: Condens. Matter* **9** 7359
- [22] Held K *et al* 2006 *Phys. Status Solidi B* **243** 2599
- [23] Ushakov A V, Shorikov A O, Anisimov V I, Baranov N V and Streltsov S V 2017 *Phys. Rev. B* **95** 205116
- [24] Skorikov N A, Shorikov A O, Skornyakov S L, Korotin M A and Anisimov V I 2015 *J. Phys.: Condens. Matter* **27** 275501
- [25] Perdew J P, Burke K and Ernzerhof M 1996 *Phys. Rev. Lett.* **77** 3865
- [26] Giannozzi P *et al* 2009 *J. Phys.: Condens. Matter* **21** 395502
- [27] Korotin D, Kozhevnikov A V, Skornyakov S L, Leonov I, Binggeli N, Anisimov V I and Trimarchi G 2008 *Eur. Phys. J. B* **65** 91
- [28] Lichtenstein A I and Katsnelson M I 1998 *Phys. Rev. B* **57** 6884
- [29] Gull E, Millis A J, Lichtenstein A I, Rubtsov A N, Troyer M and Werner P 2011 *Rev. Mod. Phys.* **83** 349
- [30] Poteryaev A, Belozerov A, Dyachenko A, Korotin D, Korotin M, Shorikov A, Skorikov N, Skornyakov S and Streltsov S AMULET <http://amulet-code.org>
- [31] Vidberg H J and Serene J E 1977 *J. Low Temp. Phys.* **29** 179
- [32] Skornyakov S L, Efremov A V, Skorikov N A, Korotin M A, Izyumov Y A, Anisimov V I, Kozhevnikov A V and Vollhardt D 2009 *Phys. Rev. B* **80** 092501
- [33] Skornyakov S L, Anisimov V I, Vollhardt D and Leonov I 2018 *Phys. Rev. B* **97** 115165
- [34] Dyachenko A A, Shorikov A O, Lukoyanov A V and Anisimov V I 2012 *JETP Lett.* **96** 56–60
- [35] Shorikov A O, Lukoyanov A V, Anisimov V I and Savrasov S Y 2015 *Phys. Rev. B* **92** 035125
- [36] Aichhorn M, Purovskii L, Vildosola V, Ferrero M, Parcollet O, Miyake T, Georges A and Biermann S 2009 *Phys. Rev. B* **80** 085101
- [37] Werner P, Gull E, Troyer M and Millis A J 2008 *Phys. Rev. Lett.* **101** 166405
- [38] Watson M D, Kim T K, Haghighirad A A, Blake S F, Davies N R, Hoesch M, Wolf T and Coldea A I 2015 *Phys. Rev. B* **92** 121108
- [39] Shorikov A, Korshunov M M and Anisimov V I 2011 *JETP Lett.* **93** 80–5